Loss of β-adrenergic–stimulated phosphorylation of Ca$_V$1.2 channels on Ser1700 leads to heart failure

Linghai Yang[a], Dao-Fu Dai[b], Can Yuan[a], Ruth E. Westenbroek[a], Haijie Yu[a], Nastassya West[c], Horacio O. de la Iglesia[c], and William A. Catterall[a,1]

[a]Department of Pharmacology, University of Washington, Seattle, WA 98195; [b]Department of Pathology, University of Washington, Seattle, WA 98195; and [c]Department of Biology, University of Washington, Seattle, WA 98195

L-type Ca^{2+} currents conducted by voltage-gated calcium channel 1.2 (Ca$_V$1.2) initiate excitation–contraction coupling in the heart, and altered expression of Ca$_V$1.2 causes heart failure in mice. Here we show unexpectedly that reducing β-adrenergic regulation of Ca$_V$1.2 channels by mutation of a single PKA site, Ser1700, in the proximal C-terminal domain causes reduced contractile function, cardiac hypertrophy, and heart failure without changes in expression, localization, or function of the Ca$_V$1.2 protein in the mutant mice (SA mice). These deficits were aggravated with aging. Dual mutation of Ser1700 and a nearby casein-kinase II site (Thr1704) caused accelerated hypertrophy, heart failure, and death in mice with these mutations (STAA mice). Cardiac hypertrophy was increased by voluntary exercise and by persistent β-adrenergic stimulation. PKA expression was increased, and PKA sites Ser2808 in ryanodine receptor type-2, Ser16 in phospholamban, and Ser23/24 in troponin-I were hyperphosphorylated in SA mice, whereas phosphorylation of substrates for calcium/calmodulin-dependent protein kinase II was unchanged. The Ca^{2+} pool in the sarcoplasmic reticulum was increased, the activity of calcineurin was elevated, and calcineurin inhibitors improved contractility and ameliorated cardiac hypertrophy. Cardio-specific expression of the SA mutation also caused reduced contractility and hypertrophy. These results suggest engagement of compensatory mechanisms, which initially may enhance the contractility of individual myocytes but eventually contribute to an increased sensitivity to cardiovascular stress and to heart failure in vivo. Our results demonstrate that normal regulation of Ca$_V$1.2 channels by phosphorylation of Ser1700 in cardiomyocytes is required for cardiovascular homeostasis and normal physiological regulation in vivo.

calcium channel | heart failure | excitation–contraction coupling | PKA | casein kinase II

Excitation–contraction (EC) coupling in the heart is initiated by L-type calcium (Ca^{2+}) currents conducted by voltage-gated calcium 1.2 (Ca$_V$1.2) channels that are activated by membrane depolarization (1). Ca^{2+} influx via Ca$_V$1.2 channels activates Ca^{2+} release from the sarcoplasmic reticulum (SR), leading to rapid and forceful contraction of myofilaments. Ryanodine receptor type-2 (RyR2) is the major channel for this release of Ca^{2+} from cardiac SR (2, 3). Mobilized Ca^{2+} is transported back into the SR by the SR Ca^{2+} ATPase (SERCA) during muscle relaxation (4). SERCA activity is controlled by the inhibitor protein phospholamban (PLB), which is phosphorylated by PKA to release its inhibition of SERCA activity (4). The force and rate of cardiac contractions are critically dependent on the amplitude and kinetics of the Ca^{2+} signal generated by Ca$_V$1.2 channels and RyR2 (1). In the fight-or-flight response, a marked increase in the beating rate and force of contraction of the heart is triggered by activation of the sympathetic nervous system and stimulation of the β-adrenergic signaling pathway. As a result, PKA is activated and phosphorylates Ca$_V$1.2, RyR2, and PLB to enhance Ca^{2+} influx, Ca^{2+} mobilization, and reuptake into the SR in cardiomyocytes, leading directly to increased contractility and contributing to the acceleration of the heart rate (3–7). PKA-mediated phosphory-

lation of Ca$_V$1.2 channels causes a three- to fourfold increase in the peak amplitude of Ca^{2+} currents in mammalian cardiomyocytes (5–7). Despite much study, the exact PKA phosphorylation sites on Ca$_V$1.2 that mediate increased channel activity in response to β-adrenergic regulation remain only partially resolved (7–9).

Cardiac Ca$_V$1.2 channels are composed of pore-forming α$_1$1.2 subunits and associated β and α$_2$δ subunits (10, 11). In skeletal muscle, an additional γ subunit is associated with the closely related Ca$_V$1.1 channels (11, 12). Multiple PKA sites have been identified by phosphorylation of purified preparations of α$_1$1.2 (Ser1928) and β (Ser459, Ser478, and Ser479) subunits; however, none of these sites is required for β-adrenergic regulation of Ca$_V$1.2 channels in cardiac myocytes in vivo or in transfected mammalian cells (7, 8). In addition to channel phosphorylation, the formation of an autoinhibitory signaling complex is also essential for β-adrenergic regulation of Ca$_V$1.2 channel activity (7, 13, 14). In skeletal and cardiac myocytes (15), as well as in neurons (16, 17), the α$_1$1.1 and α$_1$1.2 subunits are proteolytically processed at Ala1800 (or the equivalent), and the cleaved distal C terminus (dCT) is noncovalently associated with the proteolytically processed channels (13, 18). In this noncovalent complex, the dCT acts as a potent inhibitor of Ca$_V$1.2 channel activity (13). Truncated Ca$_V$1.2 channels with dCT deletion exhibit increased Ca^{2+} channel activity in transfected nonmuscle cells (13, 19), and they have reduced expression and impaired β-adrenergic regulation in vivo (20). Coexpression of the dCT with truncated Ca$_V$1.2 channels in nonmuscle cells greatly inhibits channel activity through interaction with the proximal C

Significance

Calcium entry initiates contraction in cardiac myocytes, and altered expression of voltage-gated calcium channel 1.2 (Ca$_V$1.2) causes heart failure in mice. Here we show that reducing β-adrenergic regulation of Ca$_V$1.2 by mutation of a PKA site in the C-terminal domain causes age-related heart failure. Dual mutation of a nearby casein-kinase II phosphorylation site accelerated heart failure. The PKA level was increased; PKA-mediated phosphorylation of ryanodine receptor type-2, phospholamban, and troponin-I was increased; the calcium pool in the sarcoplasmic reticulum was increased; and the activity of the calcium-dependent phosphoprotein phosphatase calcineurin was persistently elevated. These changes in mice with a mutation at the PKA site Ser1700 (SA mice) suggest that compensatory mechanisms may initially enhance contractility but eventually cause increased sensitivity to cardiovascular stress and heart failure.

---

terminus (13). The dCT also contains a leucine zipper motif that interacts with A kinase anchoring protein 15 (AKAP15) and other AKAPs to mediate PKA targeting and is required for β-adrenergic regulation of $Ca_V1.1$ and $Ca_V1.2$ channels (21, 22). This mode of regulation has been reconstituted successfully in transfected nonmuscle cells that coexpress truncated $Ca_V1.2\Delta1800$, dCT, AKAP15, $Ca_V\beta$, and $\alpha2\delta$ subunits (14). PKA activation by forskolin increased Ca^{2+} currents up to 3.6-fold compared with those observed in the presence of protein kinase inhibitors (14). In contrast, full-length $Ca_V1.2$ is not regulated by PKA activation in the same reconstituted system (14). These results suggest that β-adrenergic stimulation of $Ca_V1.2$ channel activity is mediated through disinhibition of the inhibitory effect of the dCT on proteolytically processed $Ca_V1.2$ channels.

Proteomic studies identified Ser1700 (or its equivalent) in the proximal C-terminus of $Ca_V1.1$ and $Ca_V1.2$ as a PKA phosphorylation site in skeletal and cardiac myocytes. This site is phosphorylated in vivo in response to β-adrenergic stimulation in rabbit skeletal muscle and mouse heart (23, 24). A nearby threonine (Thr1704 in $Ca_V1.2$) in a consensus sequence for casein kinase 2 (CKII) was also phosphorylated (23). In reconstituted nonmuscle cells, Ser1700 and Thr1704 are required for normal basal and PKA-regulated $Ca_V1.2$ channel activity (14). Either the $Ca_V1.2$/S1700A (SA) mutation or the $Ca_V1.2$/S1700A/ T1704A (STAA) mutation (25, 26) reduced basal $Ca_V1.2$ channel activity in cardiomyocytes, decreased β-adrenergic stimulation of channel activity and cellular contractility, and impaired exercise capacity (25, 26). Here we report that the SA and STAA mutations lead to dramatic hypertrophy with increasing age and to 100% lethal heart failure, accompanied by compensatory increases in PKA expression, hyperphosphorylation of RyR2 PLB, and troponin-I at PKA sites, increased Ca^{2+} load in the SR, and activation of a calcineurin-dependent hypertrophic pathway.

Similar effects are observed in cardiomyocyte-specific mutants. These dramatic physiological and pathophysiological consequences of the removal of a single hydroxyl group from Ser1700 highlight the importance of this regulatory site in cardiac homeostasis and physiological regulation.

Results

The S1700A Mutation in $Ca_V1.2$ Leads to Heart Failure and Premature Death.
Phosphorylation at $Ca_V1.2$/Ser1700 is absent in extracts from both STAA and SA mice, as assessed by immunoblotting and immunohistochemistry with a phosphospecific antibody against phospho-$Ca_V1.2$/Ser1700 (pS1700) (Fig. 1 A and B). The protein levels of $Ca_V1.2$ are similar in these genotypes at 2 mo of age (Fig. 1A) (25, 26), although slightly reduced expression of $Ca_V1.2$ has been observed in older, healthy STAA and SA mice (25, 26). Both STAA and SA mice died prematurely as they reached ages of 6–8 mo (Fig. 1C), with STAA mice having a significantly shorter lifespan than SA mice (median survival: STAA, 264 d; SA, 386 d). No mortality was observed for WT or heterozygous mice during our 14-mo survival study.

Cardiac hypertrophy in mutant mice as measured by the ratio of heart weight (HW) to body weight (BW) was significant in 2-mo-old mice and was more dramatic at 6 mo of age in STAA mice and at 10 mo of age in SA mice ($P < 0.05$, two-way ANOVA) (Fig. 1 D–F). In contrast, mice heterozygous for STAA or SA mutations (Het) have the same heart size as WT controls (Fig. 1 D and E). This dramatic increase in cardiac hypertrophy in mutant mice was associated with congestive heart failure, as assessed by increases in lung weight normalized to BW in 10-mo-old SA mice (Fig. 1G). No difference in BW was observed between genotypes at the indicated ages, except in some 10-mo-old SA mice with end-stage heart failure, which were excluded from HW/BW analysis. At the end stage of heart failure,
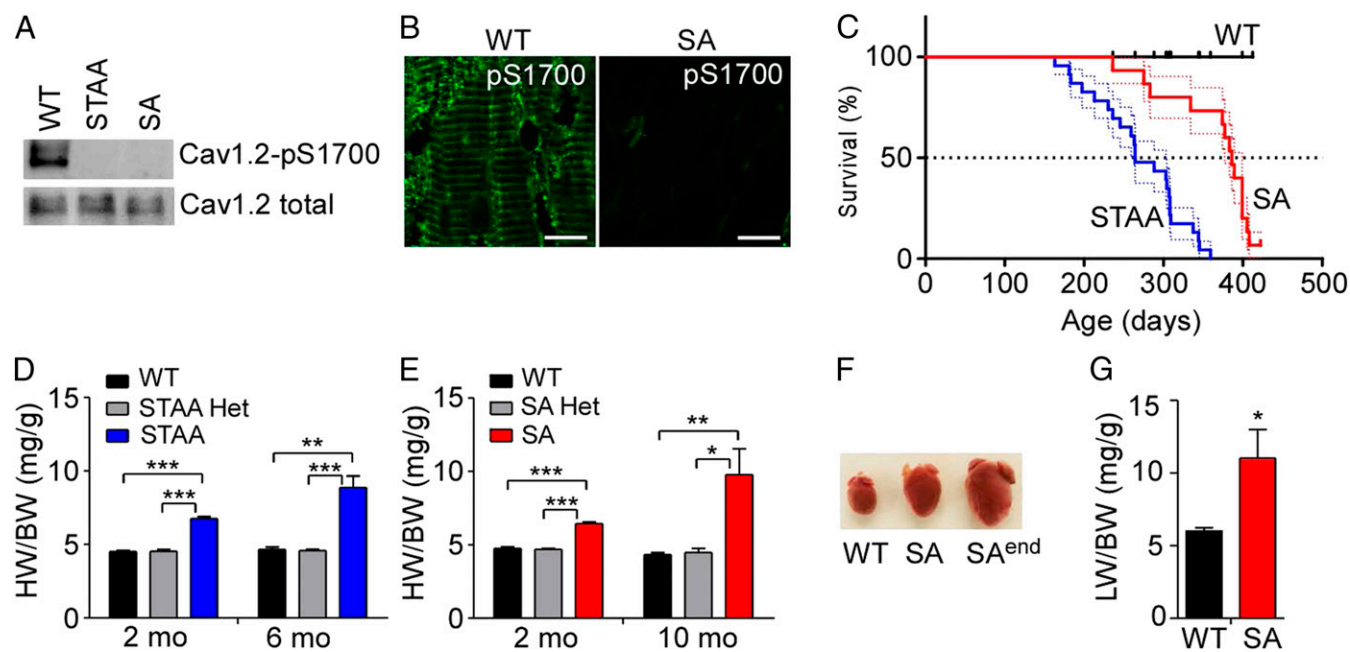

Fig. 1. Loss of phosphorylation on $Ca_V1.2$/Ser1700 leads to heart failure and premature death. (A) Immunoblot with anti–phospho-Ser1700 (pS1700)-specific antibody shows the absence of Ser1700 phosphorylation in both Cav1.2/S1700A/T1704A (STAA) and Cav1.2/S1700A) (SA) mutant mice compared with WT control. Total protein levels of $Ca_V1.2$ in the genotypes are similar at 2 mo of age. (B) Representative images of immunohistochemical staining of pS1700 in WT and SA hearts. (Scale bars: 10 μm.) (C) Kaplan–Meier survival plots of WT ($n = 14$), STAA ($n = 23$), and SA ($n = 16$) mice with aging. Log-rank test: $P < 0.05$ between SA and WT; $P < 0.001$ between STAA and WT or between STAA and SA mice. (D and E) HW/BW as a function of age in WT, STAA, and STAA Het mice (D) and in WT, SA, and SA Het mice (E) ($n = 4–11$ for each group). (F) Representative image of hearts from 10-mo-old WT and SA mice. SA^{end} shows a representative heart from an SA mouse at the end stage of heart failure. (G) Lung weight (LW)/BW of 10-mo-old WT ($n = 5$) and SA ($n = 5$) mice. *$P < 0.05$, **$P < 0.01$, ***$P < 0.001$.

both STAA and SA mice had dramatically enlarged hearts (HW:WT: 0.14 ± 0.01 g; STAA: 0.54 ± 0.05 g; SA: 0.52 ± 0.03 g, $P < 0.01$) (Fig. 1 $D–F$) and reduced BW resulting from illness. These results show that loss of Ser1700 phosphorylation on $Ca_V1.2$ causes spontaneous cardiac hypertrophy and heart failure, without changes in the expression, localization, or function of $Ca_V1.2$ (25, 26) and further indicate that loss of Thr1704 phosphorylation plays a synergistic role. In further studies, we focused primarily on the healthier SA mice, in which only PKA phosphorylation of Ser1700 is prevented.

Cardiac Performance Is Impaired in Young Adult SA Mice. We have shown previously that the contraction of isolated SA cardiomyocytes in response to β-adrenergic stimulation is only mildly decreased, suggesting that compensatory mechanisms enhance contractility despite substantially reduced $Ca_V1.2$ channel activity (25). We used echocardiography to assess cardiac structure and function in vivo in 3-mo-old WT, SA Het, and SA mice. Left ventricular systolic function measured by fractional shortening (FS) was decreased dramatically in SA mice compared with that in WT mice, whereas SA Het mice had FS percentages similar to those in WT mice (Fig. 2A). The left ventricular myocardial performance index (MPI) showed a dramatic increase in SA mice, indicating impairment of ventricular performance compared with that in WT and SA Het mice (Fig. 2B). Tissue Doppler imaging, which measures the diastolic function of the left ventricle, showed that the ratio of the early (Ea) to late (Aa) myocardial relaxation velocities (Ea/Aa) in SA mice is significantly decreased (Ea/Aa <1) compared with WT and SA Het control mice (Ea/Aa >1) (Fig. 2C). This finding indicates diastolic dysfunction in SA mice, which may be caused by stiffness of the left ventricle. There was no significant change in the left ventricular wall thickness (Fig. 2D). These results show that SA mice have significantly impaired ventricular systolic and diastolic function in young adulthood. Increases in heart size and left ventricular chamber dimensions were evident in histological analysis of SA mice at the same age (Fig. 2E). These results are consistent with our observation that 2-mo-old SA mice have an increased HW/BW ratio compared with WT and Het controls (Fig. 1E).

Elevated Sensitivity to β-Adrenergic Stimulation and Exercise-Induced Cardiac Hypertrophy in SA Mice. Chronic heart failure is associated with an increase in β-adrenergic drive, and β-adrenergic antagonists are the mainstay of treatment to improve cardiac function in patients with established chronic heart failure (27, 28). Mice chronically treated with isoproterenol also exhibit cardiac hypertrophy and heart failure (29). To examine whether SA mice have altered responses to chronic β-adrenergic stimulation, we treated SA and age-matched WT mice with isoproterenol at 3 mo of age. Using a relatively low dose of isoproterenol (10 mg·kg^{-1}·d^{-1}), we found that SA mice had a significantly greater increase in the HW/BW ratio than WT control mice (Fig. 3A). The effect of isoproterenol was completely inhibited in SA mice when coinjected with either metoprolol (a selective β1-adrenergic receptor antagonist) or carvedilol (a nonselective β-adrenergic antagonist) (Fig. 3A), suggesting that the hypertrophic effect of isoproterenol occurred mainly through β1-adrenergic activation.

Voluntary wheel-running induces cardiac hypertrophy in mice (30). To examine if SA mice have increased sensitivity to exercise-induced hypertrophy, 12-wk-old mice were singly housed with free access to a running wheel for 4 wk. The running activity and circadian patterns were similar in SA and age-matched WT mice (Fig. 3 B and C), suggesting that SA mice have normal voluntary wheel-running activity even though they had reduced maximal exercise capacity on a forced-treadmill test (25). Exercised SA mice had significantly increased HW/BW ratios compared with nonexercised age-matched SA control mice (Fig. 3D). In contrast, exercised WT mice had HW/BW ratios similar to those of nonexercised WT control mice (Fig. 3D). These results indicate that SA mice are more sensitive than WT mice to exercise-induced cardiac hypertrophy.

To examine if β-adrenergic receptor blockade has beneficial effects on cardiac function, we treated SA mice with either vehicle or metoprolol for 4 wk using s.c. osmotic minipumps. Unexpectedly, cardiac contractility of SA mice was impaired significantly by metoprolol compared with vehicle treatment, as measured by the percentage of FS (%FS) and MPI (Fig. 3 E and F). However, the left ventricular end diastolic diameter
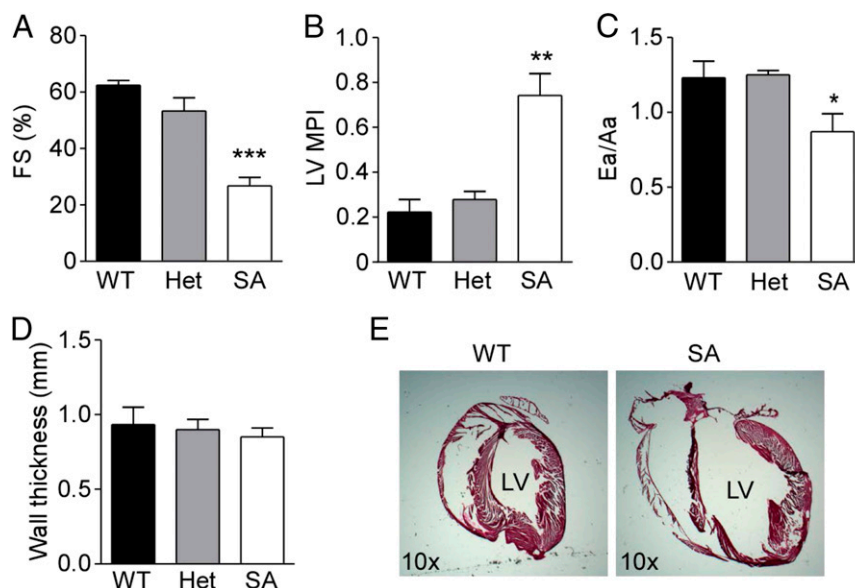

Fig. 2. SA mice exhibit impaired cardiac performance and dilated hypertrophy at 3 mo of age. ($A–D$) Echocardiographic assessment of the ventricle %FS (A), left ventricle MPI (B), the Ea/Aa diastolic velocity ratio (C), and septal and left ventricle posterior wall thickness (D) in hearts of WT ($n = 5$), Het ($n = 4$), and SA ($n = 5$) mice. (E) Representative sagittal histological sections of hearts from WT and SA mice stained with H&E. LV, left ventricle. *$P < 0.05$, **$P < 0.01$, ***$P < 0.001$ compared with WT control.
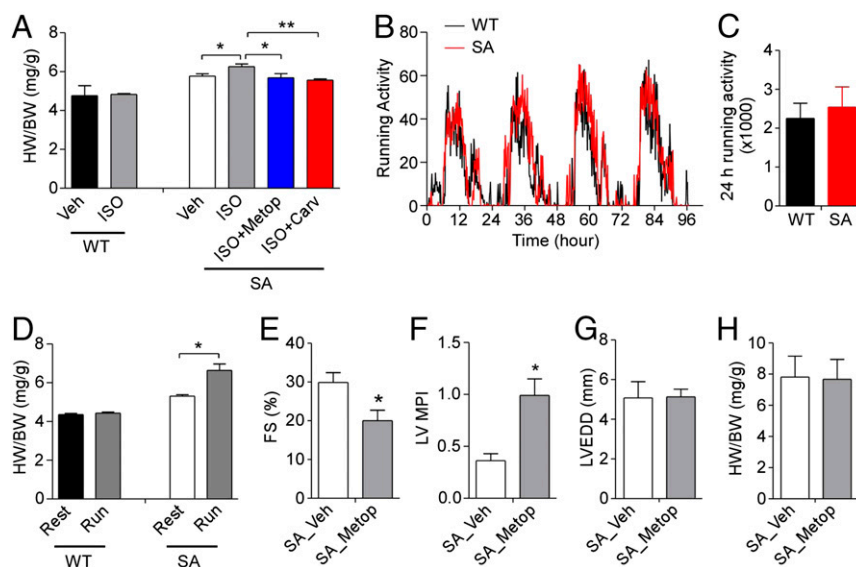
Fig. 3. Increased sensitivity to isoproterenol-induced hypertrophy and exercise in SA mice. (A) HW/BW of WT and SA mice after treatment as indicated with vehicle (Veh), isoproterenol (ISO, 10 mg·kg^{-1}·d^{-1}), isoproterenol plus metoprolol (ISO + Metop, 60 mg·kg^{-1}·d^{-1}), or isoproterenol plus carvedilol (ISO + Carv, 10 mg·kg^{-1}·d^{-1}). Mice were injected i.p. once per day for 14 consecutive days (n = 4 or 5 for each group). (B and C) Running-wheel activity of WT (n = 6) and SA (n = 6) mice during a 4-d period. (D) HW/BW of WT (n = 6) and SA (n = 6) mice with or without 4 wk of running-wheel exercise. (E–H) Echocardiographic assessment of %FS (E), LV MPI (F), LVEDD (G), and HW/BW (H) of age-matched SA mice after treatment with vehicle (Veh; n = 5) or metoprolol (Metop, 2.5 mg·kg^{-1}·h^{-1}; n = 6) for 4 wk with an s.c. Alzet osmotic minipump. *P < 0.05, **P < 0.01.

(LVEDD) and HW/BW ratio were not changed by metoprolol treatment (Fig. 3 G and H). These results indicate that β-receptor blockade has a detrimental effect on cardiac contractility in 3-mo-old SA mice and has no beneficial effect on cardiac hypertrophy at that early stage of their heart failure.

PKA-Dependent Compensatory Changes in SA Mice. The contractility of SA cardiomyocytes was largely preserved despite severely reduced basal and β-adrenergic–stimulated L-type Ca^{2+} current (25), suggesting the engagement of cellular compensatory mechanisms favoring contraction. Because cytoplasmic Ca^{2+} transients are required for contraction, a possible mechanism is that SA cardiomyocytes may have increased intracellular Ca^{2+} release from the SR through RyR2 channels, whose activity is increased after PKA-mediated phosphorylation at Ser2808 (31). We found that both the level of expression of the PKA catalytic subunit Cα and the level of phosphorylation of RyR2 at Ser2808 were increased significantly in the hearts of SA mice compared with WT controls (Fig. 4 A and B), suggesting that the increases in PKA activity and RyR2 activity might contribute to the preservation of cardiac contractility in SA mice. In addition, phosphorylation of PKA regulatory sites in PLB (Ser16) and troponin-I (Ser23/24) was also increased, consistent with the increased level of PKA expression (Fig. 4 C and D). In contrast, phosphorylation by calcium/calmodulin-dependent protein kinase II at Ser2814 in RyR2 and Thr17 in PLB was not increased, suggesting specific hyperactivation of the PKA-signaling pathway (Fig. 4 C and D).

Increased SR Calcium, Hyperactivated Calcineurin, and Improvement in Cardiac Performance by Calcineurin Inhibition in SA Mice. Increased phosphorylation of PLB at Ser16 would relieve the inhibition of SERCA2 and increase pumping of Ca^{2+} into the SR (4). Consistent with this effect, we found that SA mice have increased Ca^{2+} load in the SR, as determined from Ca^{2+} imaging of the release of SR content by activation of RyR2 with caffeine and inhibition of SERCA with thapsigargin (Fig. 5). Increased Ca^{2+} in the SR and increased Ca^{2+} release via RyR2 activated by phosphorylation of Ser2808 leads to activation of the

Ca^{2+}/calmodulin-dependent phosphoprotein phosphatase calcineurin and downstream signaling to the nuclear factor of activated T cells (NFAT) pathway, which in turn is sufficient to cause cardiac hypertrophy if chronically activated (32). Consistent with their cardiac hypertrophy, SA mice have significantly increased calcineurin phosphatase activity in their hearts compared with WT control mice (Fig. 6A). Furthermore, SA mice treated for 2 wk with the calcineurin inhibitor FK-506 exhibited significantly improved cardiac function compared with vehicle-treated controls (Fig. 6 B–D). Similarly, SA mice treated with either FK-506 or the calcineurin inhibitor cyclosporine A (CsA) showed significant regression of cardiac hypertrophy as measured by the HW/BW ratio (Fig. 6 E and F). These data suggest that the persistent compensatory increases in PKA, SERCA, and RyR2 activity in SA cardiomyocytes eventually lead to calcineurin activation and cardiac hypertrophy.

Cardiomyocyte-Specific Expression of the SA Mutation Leads to Cardiac Hypertrophy and Impaired Contractility. Ca$_V$1.2 is also expressed in vascular smooth muscle, autonomic neurons, and endocrine cells. To exclude effects of the SA mutation in these other cell types, we generated mice with cardiomyocyte-specific expression of the SA mutation. By crossing SA mice (Ca$_V$1.2$^{SA/SA}$) with transgenic mice expressing tamoxifen-inducible Cre recombinase under the control of the α-myosin heavy-chain promoter (αMHC-MerCreMer, herein referred to as "Cre") and Ca$_V$1.2$^{lox/lox}$ mice (33, 34), we obtained Cre;Ca$_V$1.2$^{SA/lox}$ and control Cre;Ca$_V$1.2$^{WT/lox}$ mice. After tamoxifen treatment, the floxed Ca$_V$1.2 allele was inactivated selectively in cardiomyocytes, leaving only one mutant SA allele expressed in Cre;Ca$_V$1.2$^{SA/lox}$ mice and one WT allele expressed in control Cre;Ca$_V$1.2$^{WT/lox}$ mice. In other tissues, both WT and SA alleles were expressed heterozygously in Cre;Ca$_V$1.2$^{SA/lox}$ mice. Based on our results (Figs. 1E and 2), SA/WT heterozygosity had no effect on cardiac function. As shown in Fig. 7 A and B, tamoxifen treatment inactivated the floxed Ca$_V$1.2 allele and substantially reduced the level of phosphorylated Ser1700 in heart extracts from Cre;Ca$_V$1.2$^{SA/lox}$ mice. As expected, the levels of phosphorylated Ser1700 in
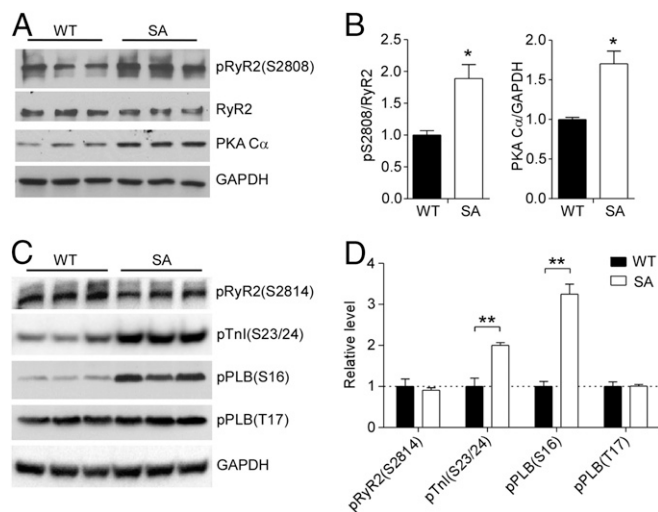
Fig. 4. PKA-dependent compensatory changes in expression and phosphorylation in SA mice. (*A* and *B*) Immunoblots (*A*) and quantification (*B*) of phosphorylation of RyR at Ser2808 (pS2808) and the PKA Cα subunit in 3-mo-old WT and SA mice. Total RyR2 and GAPDH were used as loading controls. *$P < 0.05$ versus WT. $n = 5$ for each genotype. (*C* and *D*) Immunoblots (*C*) and quantification (*D*) of phosphorylation of RyR2 at S2814, troponin-I at S23/24, and PLB at S16 and T17 in ventricular lysates of 3-mo-old WT and SA mice. Total GAPDH was used as a loading control. $n = 3$ for each genotype. *$P < 0.05$; **$P < 0.01$.

cardiac samples from untreated Cre;Ca$_V$1.2$^{SA/lox}$ mice and tamoxifen-treated Cre;Ca$_V$1.2$^{WT/lox}$ mice were comparable, because in both groups only one WT Ca$_V$1.2 allele was expressed, whereas the untreated Cre;Ca$_V$1.2$^{WT/lox}$ mice expressed both WT alleles and had significantly more phosphorylated Ser1700 (Fig. 7*B*). The remaining phosphorylated Ser1700 in samples from tamoxifen-treated Cre;Ca$_V$1.2$^{SA/lox}$ mice (27 ± 1.6% of the untreated control) likely reflects Ca$_V$1.2 in vascular smooth muscle and autonomic neurons resident in the heart, plus incomplete Cre-mediated recombination in the myocytes [80% recombination efficiency as reported (33)]. These results indicate that the tamoxifen-treated Cre;Ca$_V$1.2$^{SA/lox}$ mouse can be used as a model for cardiomyocyte-specific expression of the Ca$_V$1.2/S1700A mutation.

Echocardiographic analysis of Cre;Ca$_V$1.2$^{SA/lox}$ mice 4 wk after tamoxifen treatment revealed decreased ventricular contraction as measured by %FS (Fig. 7*C*) and impaired systolic/diastolic function as shown by increased MPI (Fig. 7*D*), without significant effects on the Ea/Aa ratio (Fig. 7*E*) or LVEDD (Fig. 7*F*), compared with those in tamoxifen-treated Cre;Ca$_V$1.2$^{WT/lox}$ mice. Consistent with the impaired cardiac performance, tamoxifen-treated Cre;Ca$_V$1.2$^{SA/lox}$ mice showed an increased HW/BW ratio compared with that in Cre;Ca$_V$1.2$^{WT/lox}$ mice or Cre-negative Ca$_V$1.2$^{SA/lox}$ mice treated with tamoxifen (Fig. 7*G*). In vehicle-treated mice, there was no difference in the HW/BW ratios of the different genotypes (Fig. 7*G*). The increased heart size after tamoxifen treatment in Cre;Ca$_V$1.2$^{SA/lox}$ mice is also evident by histological analysis (Fig. 7*H*). These results indicate that the hypertrophic effect was caused by tamoxifen and Cre-induced expression of the SA mutation in cardiomyocytes rather than by cardiac toxicity of tamoxifen-induced Cre activity in cardiomyocytes, as has been observed previously with higher doses of tamoxifen (35). Evidently, the SA mutation is sufficient to impair cardiovascular homeostasis and cause cardiac hypertrophy within 4 wk when expressed only in cardiomyocytes.

Discussion

Our results advance the knowledge of Ca$_V$1.2 channel regulation and heart failure in four important ways. First, we report that partial block of β-adrenergic regulation of cardiac Ca$_V$1.2 channels in SA and STAA mice per se is sufficient to cause dramatic hypertrophy and heart failure, without effects on the expression, localization, or function of Ca$_V$1.2 channels in cardiac myocytes. Second, we show that phosphorylation of the PKA site Ser1700 is crucial for both cardiovascular homeostasis and prevention of heart failure, as well as for normal basal levels of Ca$_V$1.2 channel activity and normal up-regulation by β-adrenergic/PKA signaling. Third, we find that phosphorylation of the CKII site Thr1704 contributes to both cardiovascular homeostasis and prevention of heart failure as well as to normal basal levels of Ca$_V$1.2 channel activity and normal up-regulation by β-adrenergic/PKA signaling. Fourth, our results indicate that the cardiac hypertrophy and heart failure initiated by mutation of Ser1700 induce compensatory up-regulation of PKA expression,
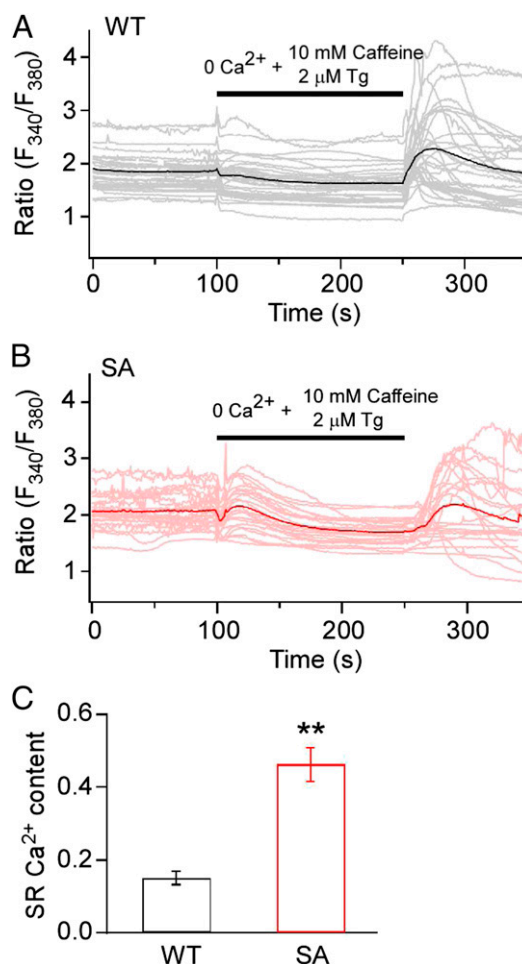

Fig. 5. Increased Ca^{2+} load in the SR of ventricular myocytes from SA mice. (*A*) WT mice. (*B*) SA mice. Ca^{2+}-transients were evoked by depletion of the SR store and subsequent reperfusion-induced Ca^{2+} entry. SR store depletion was evoked by perfusion of 10 mM caffeine plus 2 μM thapsigargin in the absence of extracellular Ca^{2+} (black bars). Representative traces of Ca^{2+} concentration demonstrating the time course of SR store depletion and subsequent store-operated Ca^{2+} entry in individual ventricular myocytes are shown as lighter traces. The dark trace is the average of the lighter traces that represent the single-cell responses. For each trace, the fluorescent signal at the end of store depletion was subtracted from the fluorescent signal at the beginning of store depletion so that each cell served as its own control. This procedure eliminates the effects of individual variation in the absolute value of the fluorescent signal and allows calculation of mean ± SEM for SR calcium load with good accuracy and reproducibility as reflected in *C*. (*C*) Quantitative comparison of SR store showing the average change during SR depletion process as mean ± SEM. **$P < 0.01$.
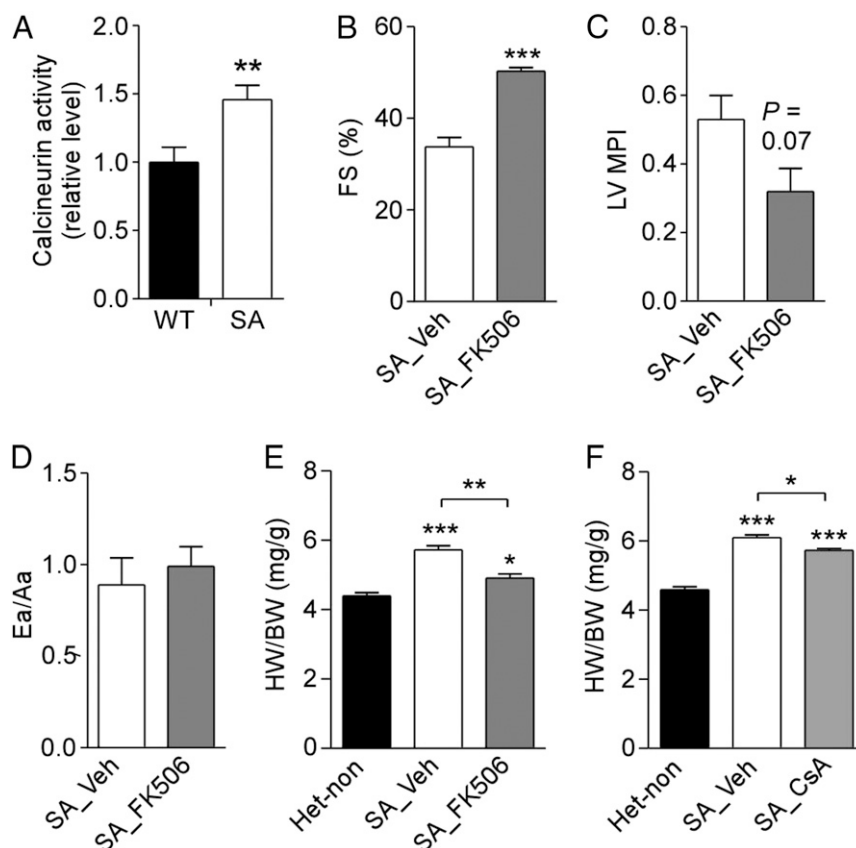
Fig. 6. Calcineurin-dependent hypertrophy in SA mice. (*A*) Calcineurin phosphatase activity from the hearts of 2-mo-old WT and SA mice. Calcineurin activity was normalized to the WT group. $n = 6$ for each genotype. (*B–D*) Echocardiographic assessment of %FS (*B*), left ventricle MPI (*C*), and Ea/Aa ratio (*D*) in 6- to 8-wk-old SA mice treated twice daily for 14 d with vehicle ($n = 4$) or FK-506 (3 mg·kg^{-1}·d^{-1}; $n = 5$). (*E*) HW/BW in untreated Het control ($n = 5$) and SA mice treated with vehicle ($n = 4$) or FK-506 ($n = 5$) in *B–D*. Mice were killed after echocardiographic analysis, and ventricular weights were measured. (*F*) HW/BW in 12-wk-old nontreated Het control mice ($n = 3$) and SA mice treated twice daily for 14 d with vehicle ($n = 5$) or CsA 15 mg/kg ($n = 5$). *$P < 0.05$, **$P < 0.01$, ***$P < 0.001$.

hyperphosphorylation of Ser16 on PLB, of Ser2808 on RyR2, and of Ser23/24 on troponin-I, and increased Ca^{2+} loading of the SR. Although compensatory up-regulation of PKA and hyperphosphorylation of downstream targets are initially effective in sustaining contractility, this persistent activation of cAMP and Ca^{2+}-signaling pathways eventually leads to heart failure via hyperstimulation of calcineurin and its downstream signaling to the nucleus via NFAT. These conclusions are considered in more detail below.

Expression and Regulation of Ca$_V$1.2 Channels in SA and STAA Mice.
Interpreting our results in terms of the regulation of Ca$_V$1.2 channels requires that the mutant channels be expressed at normal levels and localized at the cell surface in cardiac myocytes in vivo. In our first mouse model of the regulation of Ca$_V$1.2 channels we deleted the entire distal C-terminal domain (20). Those mice died from perinatal heart failure. Using quantitative immunocytochemical methods, we found that Ca$_V$1.2 channel expression in ventricular myocytes was greatly reduced on embryonic day 18 (20). Similarly, in cardiac myocytes cultured from mutant mice on the same day, recordings of gating charge movement also showed a large decrease in Ca$_V$1.2 channels on the cell surface (20). Moreover, the Ca$_V$1.2 channels that were expressed had completely lost their ability to be regulated by the activation of PKA signaling with forskolin (20). These results showed that the distal C-terminal domain is required for normal expression of Ca$_V$1.2 channels in ventricular myocytes and for regulation by the PKA pathway. Importantly, these results also established that the immunocytochemical methods we used could

detect quantitative changes in expression and localization of Ca$_V$1.2 channels.

The functional role of phosphorylation of Ser1700 and Thr1704 was first revealed in reconstitution experiments in human embryonic kidney tsA-201 cells (14). In these cells, expression of Ca$_V$1.2 channels at the cell surface was assessed from measurements of gating currents, and regulation by PKA was studied in parallel measurements of Ba^{2+} currents. Mutation of Ser1700 and Thr1704 individually or together had no effect on cell-surface expression of Ca$_V$1.2 (14). However, basal Ca$_V$1.2 activity was substantially reduced by mutation of Ser1700 and Thr1704, and PKA-stimulated Ca$_V$1.2 channel activity was completely blocked by mutation of Ser1700. These results showed that phosphorylation of Ser1700 and Thr1704 strongly regulates basal and PKA-stimulated levels of Ca$_V$1.2 current, but mutations that prevent phosphorylation have no effect on the cell-surface expression of these channels.

Based on these results in reconstituted nonmuscle cells, we constructed SA and STAA mice having mutation of Ser1700 or of Ser1700 plus Thr1704, respectively (25, 26). Ventricular myocytes from these mice have normal (>90%) levels of expression of Ca$_V$1.2 channels at the cell surface as assessed by quantitative immunocytochemistry (25, 26), using the same experimental approach that clearly detected loss of expression of Ca$_V$1.2 channels when the distal C terminus was deleted (20). Similarly, immunoblotting did not detect reduced the expression of Ca$_V$1.2 in the experiments presented here. Thus, we conclude that mutation of Ser1700 and Thr1704 individually or together
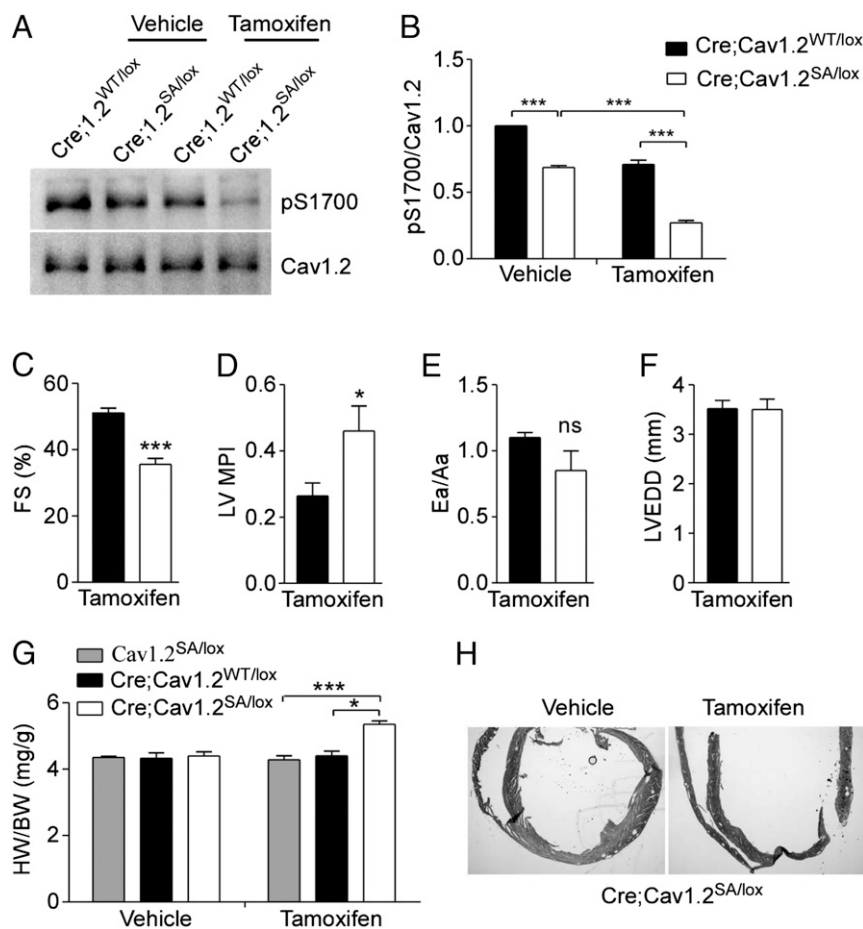
Fig. 7. Mice with the cardiomyocyte-specific SA mutation show cardiac hypertrophy and impaired ventricular performance. (*A* and *B*) Immunoblot (*A*) and quantitation (*B*) of phosphorylation of Ca$_V$1.2 at Ser1700 (pS1700) in heart lysates from mice 10 d after starting treatment with vehicle (Veh) or tamoxifen (TAM, 30 mg/kg) i.p. once daily for three consecutive days. *n* = 3 for each genotype. (*C*–*F*) Echocardiographic assessment of %FS (*C*), left ventricle MPI (*D*), Ea/Aa (*E*), and LVEDD (*F*) of αMHC-MerCreMer (Cre);Cav1.2$^{WT/lox}$ (*n* = 5) and Cre;Cav1.2$^{SA/lox}$ (*n* = 6) mice 4 wk after tamoxifen treatment. (*G*) HW/BW of the indicated genotypes 5 wk after treatment with vehicle or tamoxifen (*n* = 5–10 for each group). (*H*) H&E staining of histological sections of hearts of Cre;Cav1.2$^{SA/lox}$ mice 5 wk after vehicle or tamoxifen treatment. *$P < 0.05$, ***$P < 0.001$.

does not alter cell-surface expression of Ca$_V$1.2 in ventricular myocytes in vivo.

Because cell-surface expression is unchanged, reduced Ca$_V$1.2 currents in ventricular myocytes must reflect reductions in channel activity. In both SA mice and STAA mice, we found that the basal Ca$_V$1.2 current was reduced by ∼65% (25, 26). These results showed that the basal activity of Ca$_V$1.2 channels in ventricular myocytes depends on the phosphorylation of these two residues, as we observed in reconstituted nonmuscle cells (14). Similarly, we found that the increment in β-adrenergic–stimulated Ca$_V$1.2 current was reduced by 67% [19.4 picoampere/picofarad (pA/pF) for WT mice vs. 6.5 pA/pF for SA mice (25)]. These results support the conclusion that two-thirds of the β-adrenergic–stimulated Ca$_V$1.2 current depends on the phosphorylation of Ser1700, whereas one-third involves a separate mechanism and potentially additional phosphorylation sites (25).

Measurements of β-adrenergic stimulation of Ca$_V$1.2 current traditionally have relied on calculation of the ratio of stimulated current [S+B] over basal current (B), where S is the increment of Ca$_V$1.2 current caused by β-adrenergic stimulation. However, inhibition of protein kinases in ventricular myocytes with a broad-spectrum inhibitor reduces basal Ca$_V$1.2 current by 50–60% (36). In this situation, use of the traditional [S+B]/B ratio as a measure of β-adrenergic regulation is potentially misleading because the denominator B is not a fixed quantity. Mutations

that preferentially reduce basal current will reduce B and paradoxically will make the [S+B]/B ratio larger. Similarly mutations that affect basal and stimulated Ca$_V$1.2 current, as we have shown for SA and STAA mice, will have the same effects on S and B and therefore the [S+B]/B ratio will remain approximately unchanged even though large changes in the magnitude of β-adrenergic–stimulated Ca$_V$1.2 current may have occurred. On the other hand, mutations that preferentially reduce β-adrenergic–stimulated Ca$_V$1.2 current will reduce S, and the [S+B]/B ratio also will be reduced; however, no mutations in Ca$_V$1.2 channels that have this specific functional effect on stimulated Ca$_V$1.2 currents have been found to date. Our results suggest that the same phosphorylation sites that are involved in regulation of basal Ca$_V$1.2 currents, as assessed with broad-spectrum kinase inhibitors (36), are also involved in up-regulation by β-adrenergic stimulation, as we have observed for Ser1700 and Thr1704 (14, 25, 26). In fact, there may not be any regulatory sites that are completely unphosphorylated under basal conditions and that are phosphorylated only in response to β-adrenergic stimulation in ventricular myocytes.

β-Adrenergic regulation of the Ca$_V$1.2 current also has been analyzed in a transgenic mouse model in which exogenous WT or mutant Ca$_V$1.2 channels were studied after the expression of the transgene was induced with doxycyclin (9). Because Ca$_V$1.2 is expressed from a transgene that lacks the regulatory sequences

present in the native gene and its transcribed mRNA, control of channel expression, localization, subunit composition, and association with regulatory proteins may be altered. Moreover, in this model, the basal level of $Ca_V1.2$ current is determined by the level of induced transgene expression of $Ca_V1.2$ and therefore cannot be studied easily as an independent physiological parameter. In this experimental setting, measurements of the traditional [S+B]/B ratio did not reveal effects of Ser1700 or Thr1704 mutation, in apparent disagreement with our work (9). However, as noted above, the [S+B]/B ratio in ventricular myocytes did not change very much with the Ser1700 and Thr1704 mutations in our hands either, because these mutations reduce both the basal and the stimulated $Ca_V1.2$ current to comparable extents (25, 26). If the physiologically relevant sites for β-adrenergic stimulation of $Ca_V1.2$ current are partially phosphorylated under basal physiological conditions, it would be difficult to identify them by mutation when using a method that relies on measurements of the traditional [S+B]/B ratio because both S and B would change together, obscuring significant effects.

β-Adrenergic Regulation of Cardiac $Ca_V1.2$ Channels per se Is a Tipping Point in Heart Failure. Increased Ca^{2+} influx via $Ca_V1.2$ channels in cardiomyocytes has been proposed to be responsible for cardiac hypertrophy and pathological remodeling of the ventricles in both animal models and human patients (27, 28, 37–39). In keeping with these results, overexpression of $Ca_V1.2$ channels in the hearts of transgenic mice leads to cardiac hypertrophy and heart failure (40). Moreover, $Ca_V1.2$ blockers effectively inhibit cardiac remodeling and prevent cardiomyopathy in animal models with pressure overload (41, 42). Paradoxically, in light of these experimental results, decreased expression of $Ca_V1.2$ protein in the heart also leads to heart failure (43). In addition to direct effects on Ca^{2+} signaling, changes in $Ca_V1.2$ protein levels also would alter subcellular dyadic structures in cardiomyocytes that depend on the presence of the $Ca_V1.2$ protein (44–46) and would modify the level and composition of the supramolecular complex of $Ca_V1.2$ with other signaling proteins such as the β2-adrenergic receptor, AKAPs, adenylyl cyclases, PKA and other kinases, phosphodiesterases, and phosphoprotein phosphatases, including calcineurin (47–49). Therefore, altered expression of $Ca_V1.2$ protein could cause heart failure, or exacerbate it, by cell biological changes in subcellular membrane compartments or macromolecular signaling complexes as well as by altered Ca^{2+} signaling.

In contrast to this previous work, we specifically disrupted β-adrenergic regulation of $Ca_V1.2$ channels by protein phosphorylation without changes in channel expression, localization, or function (25, 26), and we probed the pathophysiological effects of these specific regulatory changes through studies of cardiac hypertrophy and heart failure. Remarkably, mutation of a single PKA substrate residue in $Ca_V1.2$, Ser1700, which removes only its hydroxyl group, induces dramatic cardiac hypertrophy and 100% lethal heart failure in mice. These results demonstrate the exceptional sensitivity of the heart to even partial disruption of the normal up-regulation of $Ca_V1.2$ channels by phosphorylation of Ser1700 by the β-adrenergic/PKA signaling pathway. Surprisingly, the SA mutation leads to a greater decrease in Ca^{2+} current in isolated adult cardiomyocytes than did cardiomyocyte-specific deletion of $Ca_V1.2$ in previous studies, but SA mice have less impairment of cardiac function and live much longer than cardiomyocyte-specific $Ca_V1.2$-knockout mice (compare refs. 24 and 43 and Fig. 1C). This comparison suggests that mechanisms in addition to decreased Ca^{2+} influx contribute to heart failure in mice having decreased $Ca_V1.2$ protein. Therefore, our results provide direct evidence that loss of cardiac $Ca_V1.2$ channel regulation per se is sufficient to induce cardiac hypertrophy and heart failure without changes in channel expression or localization.

Phosphorylation of Ser1700 Is Crucial for β-Adrenergic Regulation and Cardiac Homeostasis. Ser1700 (or its equivalent) is phosphorylated in vivo in response to β-adrenergic stimulation in skeletal and cardiac muscle (23, 24) and is required for the normal β-adrenergic/PKA–stimulated increase in $Ca_V1.2$ channel activity in transfected cells and in cardiac myocytes (14, 25, 26). The experiments presented here show that phosphorylation of this site is required for cardiac homeostasis and the prevention of heart failure in vivo. The mechanism of β-adrenergic/PKA stimulation of $Ca_V1.2$ channel activity in the fight-or-flight response has been controversial (7–9). However, the results of our previous experiments and those presented here leave no doubt about the importance of phosphorylation of Ser1700 in cardiovascular homeostasis and function. Mutation of this serine residue reduces basal L-type calcium current and impairs β-adrenergic/PKA stimulation of $Ca_V1.2$ channels in transfected cells and cardiac myocytes (14, 25, 26). Moreover, mutation of Ser1700 leads to dramatic cardiac hypertrophy and 100% lethal heart failure in vivo. Together, these results demonstrate clearly that phosphorylation of Ser1700 is crucial in cardiovascular regulation and homeostasis.

Phosphorylation of the CKII Site Thr1704 Enhances β-Adrenergic Regulation and Contributes to Cardiac Homeostasis. The substantially shorter lifespan of STAA mice compared with SA mice (Fig. 1C) shows that phosphorylation of Thr1704 acts synergistically with phosphorylation of Ser1700 in cardiac regulation in vivo. We found that ~25% of isolated STAA cardiomyocytes exhibited contraction failure or arrhythmic contractions in response to β-adrenergic stimulation (26); these deficits were not observed in SA cardiomyocytes (25). In STAA cardiomyocytes, but not in SA cardiomyocytes, the IC_{50} for isoproterenol stimulation of $Ca_V1.2$ activity is approximately fivefold higher than that in WT cardiomyocytes, suggesting that phosphorylation of Thr1704 and Ser1700 acts synergistically in the regulation of $Ca_V1.2$ channels in cardiomyocytes (25). Evidently, loss of this synergistic regulation in STAA mice has dire consequences for contractility, arrhythmia, and premature death. Interestingly, synergistic regulation by PKA- and CKII-mediated phosphorylation has been identified for other protein targets (50).

Mutation of Ser1700 Initiates a PKA-Dependent Compensatory Response. Cardiac myocytes from SA mice have a mild impairment in contractility, despite their major deficit in basal and β-adrenergic–stimulated Ca^{2+} currents (25), suggesting a compensatory response that increases the sensitivity of contraction to Ca^{2+} entry via $Ca_V1.2$ channels. Our experiments presented here show that PKA expression is increased and three key downstream regulatory targets of PKA are hyperphosphorylated. Increased PKA phosphorylation of PLB Ser16 would increase SERCA pumping activity and increase the pool of Ca^{2+} in the SR (4). Ca^{2+} imaging studies indicate that the level of Ca^{2+} in the SR is indeed increased in SA mice. In this context, increased PKA phosphorylation of RyR2 on Ser2808 would increase Ca^{2+} release from the SR (3). This increased Ca^{2+} would have increased effectiveness in activating contractions because of the hyperphosphorylation of troponin-I by PKA. Together, this series of compensatory events would lead to a substantial increase in the sensitivity of contractions to the diminished Ca^{2+} entering through $Ca_V1.2$ channels and thereby would sustain cellular contractility in the face of impaired basal and β-adrenergic–stimulated Ca^{2+} currents. However, persistent activation of this compensatory pathway causes increased sensitivity to stress and hyperactivated signaling via calcineurin, eventually leading to hypertrophy and heart failure.

SA Mice Show Increased Cardiovascular Pathology in Response to Stress. The SA mutation greatly decreases $Ca_V1.2$ channel activation by β-adrenergic stimulation but causes a much lesser reduction in the contractility of dissociated SA cardiomyocytes (25), suggesting compensation in the downstream signaling pathway. Consistent with that possibility, we show here that PKA is up-regulated and Ser2808 in RyR2 is hyperphosphorylated in SA mice. With the hyperactivation of this Ca^{2+} signaling pathway, which initially may help preserve contractility, two normally well-tolerated cardiovascular stresses, continuous treatment with isoproterenol and voluntary wheel-running, both led to significant increases in cardiac hypertrophy in SA mice. These results reveal at a mechanistic level how seemingly effective compensatory changes that preserve cardiac contractility in the short term can further endanger the heart and advance the process of cardiac hypertrophy and heart failure when they are persistent.

Calcineurin, $Ca_V1.2$, and Heart Failure. The increased calcineurin activity and the improvement of cardiac function by FK-506 and CsA treatment suggest that hyperactive calcineurin signaling causes cardiac hypertrophy and heart failure in SA mice. Calcineurin/NFAT signaling has been well documented as a prohypertrophic pathway in pathological conditions (32, 51). Calcineurin bound to the dCT of $Ca_V1.2$ channels has sequential effects in response to Ca^{2+} entry: it contributes to Ca^{2+}-dependent inactivation and opposes up-regulation by PKA on the millisecond timescale (52), and it signals through NFAT to gene transcription in the nucleus on a longer timescale (53). In mice with heterozygous cardiac knockout of $Ca_V1.2$ channels, calcineurin is hyperactivated, and its signaling to the nucleus via the NFAT pathway triggers hypertrophy and heart failure (43). The increased activation of calcineurin in these mice is potentially caused by chronically increased RyR2 activation and Ca^{2+} leak from the SR (43), as we propose here for SA mice. Our results add two crucial elements to this mechanism of heart failure. First, we show that this pathway to hypertrophy and heart failure can be engaged by specific impairment of the β-adrenergic regulation of $Ca_V1.2$ channels in cardiomyocytes per se, without effects on protein expression, localization, or function. Second, we demonstrate that up-regulation of PKA expression is potentially a key link in $Ca_V1.2$ channel dysfunction, cardiac hypertrophy, and heart failure. Because calcineurin/NFAT signaling is engaged to cause cardiac hypertrophy induced by increased $Ca_V1.2$ protein expression (32, 40), decreased $Ca_V1.2$ protein expression (43), and impaired regulation of $Ca_V1.2$ (this work), this mechanism gains increased emphasis as a common pathway leading to hypertrophy and heart failure.

Materials and Methods

Animals. The STAA and SA mouse lines were generated using standard methods as described previously (25, 26) and were backcrossed to C57BL/6J mice for more than eight generations. Conditional Cav1.2$^{lox/lox}$ (JAX 024714) and αMHC-MerCreMer (JAX 005657) mice were purchased from Jackson Laboratory and have been described previously (33, 34). Mice with heart-specific expression of the SA mutation were generated by crossing the αMHC-MerCreMer transgenic line to SA mice to obtain αMHC-MerCreMer; Cav$^{SA/WT}$ mice, which then were crossed to Cav1.2$^{lox/lox}$ mice to obtain αMHC-MerCreMer;Cav1.2$^{SA/lox}$ mice. Littermates with αMHC-MerCreMer;Cav1.2$^{WT/lox}$ and Cre-negative Cav1.2$^{SA/lox}$ genotypes were used as controls in biochemical and physiological studies. To induce αMHC-MerCreMer activation, mice were injected i.p. with tamoxifen (T5648; Sigma) once a day at 30 $mg·kg^{-1}·d^{-1}$ for three consecutive days (35). All mice used in this study were pathogen free and were housed in the University of Washington Animal Facility at constant temperature (22 °C), on 12-h light/12-h dark cycles, with ad libitum access to food and water. Mice were housed in groups (three to five mice per cage) except for running-wheel studies. The use of animals in this study was approved by the Institutional Animal Care and Use Committee at the University of Washington.

Immunoblot and Histological Analysis. Immunoblot analysis was performed using mouse ventricles snap-frozen in liquid nitrogen and stored at −80 °C. Ventricles were homogenized in lysis buffer [50 mM Tris·HCl (pH 7.4), 150 mM NaCl, 1% Triton X-100, 0.25% sodium deoxycholate, 1 mM EDTA, supplemented with protease inhibitors (Roche cOmplete ULTRA tablets) and phosphatase inhibitors (Roche PhosSTOP)]. Homogenates were centrifuged at 12,000 × g, 4 °C for 10 min, and the supernatants were used for blotting. Twenty micrograms of protein were loaded on 4–20% Tris-glycine polyacrylamide gels and transferred to nitrocellulose membranes. Antibodies against total $Ca_V1.2$ (CNC1) and $Ca_V1.2$-pS1700 were generated as described previously (14, 15). Antibodies against RyR2 (ARR-002; Alomone Labs), RyR2-pS2808 (ab59225; Abcam), PKA Cα subunit (sc-903; Santa Cruz), RyR2-pS2814 (A010-31; Badrilla), troponin-I-pS23/24 (4004; Cell Signaling), phospholamban-pS16 (A010-12; Badrilla), phospholamban-pT17 (A010-13; Badrilla), and GAPDH (AM4300; Invitrogen) were used. Immunoblots were analyzed using the NIH ImageJ program.

For histological studies, adult mice were anesthetized with isoflurane and transcardially perfused with PBS followed by ice-cold PBS-buffered 4% paraformaldehyde. Hearts were frozen in optimum cutting temperature (OCT) compound and were cryosectioned (10 μm). For gross histological examinations, sections were stained with H&E. For $Ca_V1.2$-pS1700 immunohistochemistry, sections were washed in PBS and incubated sequentially in blocking solution [1× PBS, 0.1% Tween 20 (PBST) and 10% normal goat serum] for >1 h and primary antibody (anti-pS1700, 1:200 in blocking solution) at 4 °C overnight. Sections then were washed four or five times in PBST and were incubated with goat anti-rabbit Alexa Fluor 488-labeled secondary antibody (1:1,000 in blocking solution) for 2–3 h. Sections were washed with PBST and mounted with VECTASHIELD mounting medium and coverslips. Images were collected using a Leica SL confocal microscope in the Keck Imaging Facility at the University of Washington.

Echocardiography, Drug Treatment, and Running-Wheel Exercise. For mice from all genotypes or treatment groups, anesthesia was induced with 2% isoflurane and sustained with 0.5% isoflurane. Echocardiography was performed with an Acuson CV-70 cardiovascular ultrasound system (Siemens) using standard imaging planes: M-mode, conventional and Tissue Doppler imaging as described previously (54). To test the effect of persistent β-adrenergic stimulation, 3-mo-old SA mice and age-matched WT mice were injected i.p. once daily with isoproterenol (10 $mg·kg^{-1}·d^{-1}$) or vehicle (saline) for 14 consecutive days. Two additional groups of mice were injected i.p. with isoproterenol (10 $mg·kg^{-1}·d^{-1}$) in combination with either the β1-selective blocker metoprolol (60 $mg·kg^{-1}·d^{-1}$) or the nonselective β-blocker carvedilol (10 $mg·kg^{-1}·d^{-1}$). For long-term metoprolol treatment, Alzet osmotic minipumps (2004; Durect Corp.) containing isoproterenol (2.5 $mg·kg^{-1}·h^{-1}$) or saline were surgically inserted s.c. in 3-mo-old mice under isoflurane anesthesia. At the fourth week following surgery, echocardiography was performed to assess cardiac function; then mice were killed, and the HW/BW ratio was measured. To test the effect of calcineurin inhibition on cardiac function, SA mice at 4–6 wk of age were injected s.c. with FK-506 (3 $mg·kg^{-1}·d^{-1}$) (Abcam) or vehicle twice daily for 14 consecutive days followed by echocardiographic assessment. For CsA (EMD Millipore) injection, 10-wk-old SA mice were injected s.c. with CsA (15 mg/kg) or vehicle twice daily for 14 d. For running-wheel exercise, 12-wk-old mice were housed singly with free access to a running wheel for 4 wk, and the running activity was automatically recorded. Age-matched mice housed singly without access to a running wheel were used as control.

Calcineurin Activity Assay. Calcineurin activity was measured by using the calcineurin cellular assay kit (BML-AK816; Enzo Life Sciences) according to the manufacturer's instructions. Briefly, ventricles from WT and SA mice were homogenized in the lysis buffer with the protease inhibitors provided in the kit. Homogenates were centrifuged at 10,000 × g, 4 °C for 10 min. Excess phosphate and nucleotides were removed from the supernatant extract by gel filtration. Five micrograms of protein were used for the assay. Calcineurin activity was measured as the dephosphorylation of a synthetic phosphopeptide substrate (RII peptide) in the presence or absence of EGTA. The amount of PO_4 released was determined photometrically by using the BIOMOL GREEN reagent provided in the kit. The phosphate release was normalized to the WT group to obtain relative calcineurin activity.

Statistics. Statistical analysis was performed using Prism GraphPad software. A log-rank test was performed to compare the survival curves of WT, STAA, and SA mice. The other comparisons were analyzed by two-tailed Student's t test for two comparisons and by one-way or two-way ANOVA for three or more groups. ANOVA was followed by Bonferroni posttests for multiple comparisons. Values are presented as means ± SEM. Differences were considered significant at $P < 0.05$.

1. Bers DM (2002) Cardiac excitation-contraction coupling. *Nature* 415(6868):198–205.
2. Ogawa Y, Kurebayashi N, Murayama T (1999) Ryanodine receptor isoforms in excitation-contraction coupling. *Adv Biophys* 36:27–64.
3. Kushnir A, Marks AR (2010) The ryanodine receptor in cardiac physiology and disease. *Adv Pharmacol* 59:1–30.
4. MacLennan DH, Kranias EG (2003) Phospholamban: A crucial regulator of cardiac contractility. *Nat Rev Mol Cell Biol* 4(7):566–577.
5. Reuter H (1983) Calcium channel modulation by neurotransmitters, enzymes and drugs. *Nature* 301(5901):569–574.
6. Osterrieder W, et al. (1982) Injection of subunits of cyclic AMP-dependent protein kinase into cardiac myocytes modulates Ca^{2+} current. *Nature* 298(5874):576–578.
7. Catterall WA (2015) Regulation of cardiac calcium channels in the fight-or-flight response. *Curr Mol Pharmacol* 8(1):12–21.
8. Weiss S, Oz S, Benmocha A, Dascal N (2013) Regulation of cardiac L-type Ca^{2+} channel $Ca_V1.2$ via the β-adrenergic-cAMP-protein kinase A pathway: Old dogmas, advances, and new uncertainties. *Circ Res* 113(5):617–631.
9. Yang L, et al. (2013) β-adrenergic regulation of the L-type Ca^{2+} channel does not require phosphorylation of α1C Ser1700. *Circ Res* 113(7):871–880.
10. Striessnig J (1999) Pharmacology, structure and function of cardiac L-type Ca^{2+} channels. *Cell Physiol Biochem* 9(4-5):242–269.
11. Catterall WA (2011) Voltage-gated calcium channels. *Cold Spring Harb Perspect Biol* 3(8):a003947.
12. Wu J, et al. (2015) Structure of the voltage-gated calcium channel $Ca_V1.1$ complex. *Science* 350(6267):aad2395.
13. Hulme JT, Yarov-Yarovoy V, Lin TW-C, Scheuer T, Catterall WA (2006) Autoinhibitory control of the $Ca_V1.2$ channel by its proteolytically processed distal C-terminal domain. *J Physiol* 576(Pt 1):87–102.
14. Fuller MD, Emrick MA, Sadilek M, Scheuer T, Catterall WA (2010) Molecular mechanism of calcium channel regulation in the fight-or-flight response. *Sci Signal* 3(141):ra70.
15. De Jongh KS, et al. (1996) Specific phosphorylation of a site in the full-length form of the α1 subunit of the cardiac L-type calcium channel by adenosine 3′,5′-cyclic monophosphate-dependent protein kinase. *Biochemistry* 35(32):10392–10402.
16. Hell JW, et al. (1996) N-methyl-D-aspartate receptor-induced proteolytic conversion of postsynaptic class C L-type calcium channels in hippocampal neurons. *Proc Natl Acad Sci USA* 93(8):3362–3367.
17. Hell JW, Appleyard SM, Yokoyama CT, Warner C, Catterall WA (1994) Differential phosphorylation of two size forms of the N-type calcium channel α1 subunit which have different COOH termini. *J Biol Chem* 269(10):7390–7396.
18. Hulme JT, et al. (2005) Sites of proteolytic processing and noncovalent association of the distal C-terminal domain of $Ca_V1.1$ channels in skeletal muscle. *Proc Natl Acad Sci USA* 102(14):5274–5279.
19. Wei X, et al. (1994) Modification of Ca^{2+} channel activity by deletions at the carboxyl terminus of the cardiac α1 subunit. *J Biol Chem* 269(3):1635–1640.
20. Fu Y, et al. (2011) Deletion of the distal C terminus of $Ca_V1.2$ channels leads to loss of β-adrenergic regulation and heart failure in vivo. *J Biol Chem* 286(14):12617–12626.
21. Hulme JT, Lin TW, Westenbroek RE, Scheuer T, Catterall WA (2003) β-adrenergic regulation requires direct anchoring of PKA to cardiac $Ca_V1.2$ channels via a leucine zipper interaction with A kinase-anchoring protein 15. *Proc Natl Acad Sci USA* 100(22):13093–13098.
22. Hulme JT, Ahn M, Hauschka SD, Scheuer T, Catterall WA (2002) A novel leucine zipper targets AKAP15 and cyclic AMP-dependent protein kinase to the C terminus of the skeletal muscle Ca^{2+} channel and modulates its function. *J Biol Chem* 277(6):4079–4087.
23. Emrick MA, Sadilek M, Konoki K, Catterall WA (2010) β-adrenergic-regulated phosphorylation of the skeletal muscle $Ca_{(V)}1.1$ channel in the fight-or-flight response. *Proc Natl Acad Sci USA* 107(43):18712–18717.
24. Lundby A, et al. (2013) In vivo phosphoproteomics analysis reveals the cardiac targets of β-adrenergic receptor signaling. *Sci Signal* 6(278):rs11.
25. Fu Y, Westenbroek RE, Scheuer T, Catterall WA (2014) Basal and β-adrenergic regulation of the cardiac calcium channel $Ca_V1.2$ requires phosphorylation of serine 1700. *Proc Natl Acad Sci USA* 111(46):16598–16603.
26. Fu Y, Westenbroek RE, Scheuer T, Catterall WA (2013) Phosphorylation sites required for regulation of cardiac calcium channels in the fight-or-flight response. *Proc Natl Acad Sci USA* 110(48):19621–19626.
27. Bristow MR (2000) beta-adrenergic receptor blockade in chronic heart failure. *Circulation* 101(5):558–569.
28. Lohse MJ, Engelhardt S, Eschenhagen T (2003) What is the role of β-adrenergic signaling in heart failure? *Circ Res* 93(10):896–906.
29. Balakumar P, Singh AP, Singh M (2007) Rodent models of heart failure. *J Pharmacol Toxicol Methods* 56(1):1–10.
30. Allen DL, et al. (2001) Cardiac and skeletal muscle adaptations to voluntary wheel running in the mouse. *J Appl Physiol* 90(5):1900–1908.
31. Shan J, et al. (2010) Role of chronic ryanodine receptor phosphorylation in heart failure and β-adrenergic receptor blockade in mice. *J Clin Invest* 120(12):4375–4387.
32. Molkentin JD, et al. (1998) A calcineurin-dependent transcriptional pathway for cardiac hypertrophy. *Cell* 93(2):215–228.
33. Sohal DS, et al. (2001) Temporally regulated and tissue-specific gene manipulations in the adult and embryonic heart using a tamoxifen-inducible Cre protein. *Circ Res* 89(1):20–25.
34. Seisenberger C, et al. (2000) Functional embryonic cardiomyocytes after disruption of the L-type $α_{1C}$ ($Ca_V1.2$) calcium channel gene in the mouse. *J Biol Chem* 275(50):39193–39199.
35. Bersell K, et al. (2013) Moderate and high amounts of tamoxifen in αMHC-MerCreMer mice induce a DNA damage response, leading to heart failure and death. *Dis Model Mech* 6(6):1459–1469.
36. duBell WH, Rogers TB (2004) Protein phosphatase 1 and an opposing protein kinase regulate steady-state L-type Ca^{2+} current in mouse cardiac myocytes. *J Physiol* 556(Pt 1):79–93.
37. Richard S, Leclercq F, Lemaire S, Piot C, Nargeot J (1998) Ca^{2+} currents in compensated hypertrophy and heart failure. *Cardiovasc Res* 37(2):300–311.
38. Mukherjee R, Spinale FG (1998) L-type calcium channel abundance and function with cardiac hypertrophy and failure: A review. *J Mol Cell Cardiol* 30(10):1899–1916.
39. Keung EC (1989) Calcium current is increased in isolated adult myocytes from hypertrophied rat myocardium. *Circ Res* 64(4):753–763.
40. Muth JN, Bodi I, Lewis W, Varadi G, Schwartz A (2001) A Ca^{2+}-dependent transgenic model of cardiac hypertrophy: A role for protein kinase Calpha. *Circulation* 103(1):140–147.
41. Liao Y, et al. (2005) Benidipine, a long-acting calcium channel blocker, inhibits cardiac remodeling in pressure-overloaded mice. *Cardiovasc Res* 65(4):879–888.
42. Semsarian C, et al. (2002) The L-type calcium channel inhibitor diltiazem prevents cardiomyopathy in a mouse model. *J Clin Invest* 109(8):1013–1020.
43. Goonasekera SA, et al. (2012) Decreased cardiac L-type Ca^{2+} channel activity induces hypertrophy and heart failure in mice. *J Clin Invest* 122(1):280–290.
44. Shaw RM, Colecraft HM (2013) L-type calcium channel targeting and local signalling in cardiac myocytes. *Cardiovasc Res* 98(2):177–186.
45. Scriven DR, Asghari P, Moore ED (2013) Microarchitecture of the dyad. *Cardiovasc Res* 98(2):169–176.
46. Sipido KR, Cheng H (2013) T-tubules and ryanodine receptor microdomains: On the road to translation. *Cardiovasc Res* 98(2):159–161.
47. Flynn R, Altier C (2013) A macromolecular trafficking complex composed of β2-adrenergic receptors, A-kinase anchoring proteins and L-type calcium channels. *J Recept Signal Transduct Res* 33(3):172–176.
48. Harvey RD, Hell JW (2013) $Ca_V1.2$ signaling complexes in the heart. *J Mol Cell Cardiol* 58:143–152.
49. Nikolaev VO, et al. (2010) β2-adrenergic receptor redistribution in heart failure changes cAMP compartmentation. *Science* 327(5973):1653–1657.
50. Huang G, et al. (2007) Protein kinase A and casein kinases mediate sequential phosphorylation events in the circadian negative feedback loop. *Genes Dev* 21(24):3283–3295.
51. Wilkins BJ, et al. (2004) Calcineurin/NFAT coupling participates in pathological, but not physiological, cardiac hypertrophy. *Circ Res* 94(1):110–118.
52. Dittmer PJ, Dell'Acqua ML, Sather WA (2014) Ca^{2+}/calcineurin-dependent inactivation of neuronal L-type Ca^{2+} channels requires priming by AKAP-anchored protein kinase A. *Cell Reports* 7(5):1410–1416.
53. Murphy JG, et al. (2014) AKAP-anchored PKA maintains neuronal L-type calcium channel activity and NFAT transcriptional signaling. *Cell Reports* 7(5):1577–1588.
54. Dai DF, et al. (2009) Overexpression of catalase targeted to mitochondria attenuates murine cardiac aging. *Circulation* 119(21):2789–2797.